ARMY RESEARCH LABORATORY

Modal Synthesis of a Non-Proportionally Damped, Gyroscopically Influenced, Geared Rotor System via the State-Space

by David B. Stringer, Pradip N. Sheth, and Paul E. Allaire

ARL-TR-4582 September 2008

NOTICES

Disclaimers

The findings in this report are not to be construed as an official Department of the Army position unless so designated by other authorized documents.

Citation of manufacturer's or trade names does not constitute an official endorsement or approval of the use thereof.

Destroy this report when it is no longer needed. Do not return it to the originator.

Army Research Laboratory
Adelphi, MD 20783-1197

ARL-TR-4582 **September 2008**

Modal Synthesis of a Non-Proportionally Damped, Gyroscopically Influenced, Geared Rotor System via the State-Space

David B. Stringer
Vehicle Technology Directorate, ARL

Pradip N. Sheth and Paul E. Allaire
Department of Mechanical and Aerospace Engineering, University of Virginia

REPORT DOCUMENTATION PAGE

Form Approved
OMB No. 0704-0188

1. REPORT DATE *(DD-MM-YYYY)*	2. REPORT TYPE	3. DATES COVERED (From - To)
September 2008	Final	

4. TITLE AND SUBTITLE
Modal Synthesis of a Non-Proportionally Damped, Gyroscopically Influenced, Geared Rotor System via the State-Space

5a. CONTRACT NUMBER

5b. GRANT NUMBER

5c. PROGRAM ELEMENT NUMBER

6. AUTHOR(S)
David B. Stringer, Pradip N. Sheth, and Paul E. Allaire

5d. PROJECT NUMBER

5e. TASK NUMBER

5f. WORK UNIT NUMBER

7. PERFORMING ORGANIZATION NAME(S) AND ADDRESS(ES)
U.S. Army Research Laboratory
ATTN: AMSRD-ARL-VT
NASA Glenn Research Center
Cleveland, Ohio

8. PERFORMING ORGANIZATION REPORT NUMBER
ARL-TR-4582

9. SPONSORING/MONITORING AGENCY NAME(S) AND ADDRESS(ES)

10. SPONSOR/MONITOR'S ACRONYM(S)

11. SPONSOR/MONITOR'S REPORT NUMBER(S)

12. DISTRIBUTION/AVAILABILITY STATEMENT
Approved for public release; distribution unlimited.

13. SUPPLEMENTARY NOTES

14. ABSTRACT
Modal synthesis provides for degree-of-freedom reduction and model simplification. This report presents a method for conducting modal synthesis on a geared rotor dynamic system under the influences of non-proportional damping and gyroscopic effects. Based on the familiar first-order, state-space methodology, a coordinate transformation is developed for diagonalizing the state-space equations of motion for each substructure of the system. A modal synthesis procedure then assembles the system equations of motion from the individual substructures. The coupling between the substructures occurs via the gear mesh. Using this methodology, the size and complexity of the model are reduced without incurring any significant loss in accuracy. The reduced model still allows for traditional methods of system analysis: Eigen-solution analysis, frequency domain response, and time domain response. Validation of this methodology occurs through its application to a finite element analysis of a geared system already published in the literature. The application illustrates that the results of the reduced system match almost exactly with the full finite element model. Additionally, the topics of gearing and gyroscopic effects are discussed with respect to limitations that arise from the analysis. In addition to model simplification, this technique also exhibits further potential for use in optimization and system identification schemes.

15. SUBJECT TERMS
Component mode synthesis, geared rotor dynamics, modal synthesis

16. SECURITY CLASSIFICATION OF:			17. LIMITATION OF ABSTRACT	18. NUMBER OF PAGES	19a. NAME OF RESPONSIBLE PERSON
a. REPORT	b. ABSTRACT	c. THIS PAGE			David B. Stringer
U	U	U	UU	35	19b. TELEPHONE NUMBER (*Include area code*) (216) 433-8482

Standard Form 298 (Rev. 8/98)
Prescribed by ANSI Std. Z39.18

Contents

List of Figures

List of Tables

Acknowledgments

Many thanks to Mr. Al Kascak, ARL-VTD, NASA Glenn Research Center, for his in-depth and critical review of this work. It is much appreciated.

INTENTIONALLY LEFT BLANK.

1. Background

A complex mechanical system analysis can incur several hundred, thousand, or even million degrees of freedom (DOF). As the number of DOF in the system increases, so does the computing time, in some cases exponentially. Consequently, computational engineers are always seeking to strike a balance between model accuracy and computational efficiency.

In 1960, Hurty (*1*) introduced the concept of modal synthesis, also called substructure or component mode synthesis. It has enjoyed popularity over four decades due to its straightforward methodology. The premise of modal synthesis is that the first few modes of vibration of a complex structure can be predicted by using the lower modes of vibration of its substructures (*2*). An extension of modal analysis, modal synthesis provides for a reduction in the overall number of DOF. As such, the computational complexity decreases, but the reduced model still maintains the desired numerical precision.

The theory behind modal analysis is fairly simple. A coordinate transformation of the equations of motion yields an equivalent uncoupled system of equations, each of which is linearly independent of the others. The transformation yields the equations in terms of principal coordinates rather than physical coordinates. The physical motion of the system then is simply a linear combination of the motion of the principal coordinates such as in equation 1.

$$\begin{aligned} \{q(z,t)\} &= [\varphi(z)][v(t)] \\ \{q(z,t)\} &= \varphi_1(z)v_1(t) + \varphi_2(z)v_2(t) + \ldots + \varphi_N(z)v_N(t) \end{aligned} \tag{1}$$

where $v_i(t)$ is the i^{th} principal coordinate response of the diagonalized equations of motion, and $\{\varphi_i(z)\}$ is the corresponding eigenvector or mode shape.

One benefit of modal analysis is that it shows the contribution of the individual modes of vibration to the motion of the entire structure and thus explicitly captures the dynamics of the system. The lower modes extracted by modal analysis generally provide the most contribution to the motion of the system. Therefore, it provides a basis for DOF reduction and model simplification. Using modal analysis, the following applications are available: among others, structural modification, sensitivity analysis, model reduction, correlation of model and finite element results, response prediction, substructure coupling, and structural damage detection (*3*).

In dynamic analysis, traditional modal analysis techniques have achieved varying degrees of success when a system undergoes damping, due to the presence of the damping matrix. In structural applications, the common approach is to assume proportional damping, such that traditional eigenvalue approaches still apply. In rotor dynamic applications, however, the damping is rarely, if ever, proportional.

Furthermore, the gyroscopics of a spinning rotor produce frequency variations which are absent in non-spinning systems. One of the first rotor dynamic analyses to use modal synthesis resulted in the computer program Analysis of Rotor Dynamic Systems (ARDS) that could return the frequency modes within 1-10% error (*4*). However, gyroscopic effects were not explicitly defined within the program.

While the gyroscopic forces are themselves conservative and take no energy from the system, they can become significant at higher rotational speeds and must be addressed.

The presence of gearing also complicates the modal analysis process. Separately, the scientific studies of gearing and rotor dynamics first appeared approximately 150 years at the height of the Industrial Revolution. Studied together, geared rotor dynamic models did not appear until the 1960s (*5*). Gears couple the motion of rotating shafts together and result in coupled lateral-torsional or lateral-torsional-axial vibrations not found in non-geared rotating shafts. Additionally, the gear mesh induces a periodic forcing function known as the gear-mesh, or tooth-pass, frequency. The gear-mesh frequency has a unique impact and is further discussed later.

Returning to the subject of general damping in dynamic models, previous attempts have made approximations by different methods (*6*), the most common being the proportional damping assumption. Once again, this is not particularly useful in rotor dynamics. Another approach ignores damping in the system and focuses only on the mass and stiffness contributions, resulting in the familiar eigenvalue problem: $(\mathbf{K} - \lambda^2 \mathbf{M} = \mathbf{0})$. A third method has been to transform the damping matrix via the traditional modal matrix and simply ignore the off-diagonal terms. Other methods (*7, 8*) perform an iterative procedure in transforming systems consisting of symmetric damping matrices only. However, a modal transformation does exist (*9, 10*) to uncouple the equations of motion for a system undergoing general damping that can include gyroscopic effects. This transformation procedure provides the theoretical basis for the proposed methodology.

The overarching objective of this report is to present a method for conducting modal synthesis on a geared rotor dynamic system under the influences of non-proportional damping and gyroscopic effects. In addition to model simplification, this technique also exhibits further potential for use in optimization and system identification schemes.

2. Coordinate Transformation

2.1 Theory

For a rotor dynamic system undergoing general damping and gyroscopic effects, the general equations of motion are

$$\begin{aligned}[\mathbf{M}]\{\ddot{\mathbf{q}}\}+[\mathbf{D}]\{\dot{\mathbf{q}}\}+[\mathbf{K}]\{\mathbf{q}\}&=\{\mathbf{F}(t)\}\\ [\mathbf{D}]&=[\mathbf{C}]+\Omega[\mathbf{G}]\end{aligned} \tag{2}$$

where [D] is the "damping" matrix, consisting of the general damping matrix, [C], and the skew-symmetric gyroscopic matrix, [G]. The gyroscopic effects in the system are a function of the shaft rotational speed, (Ω), and the gyroscopic matrix. This representation is often defined as the "real" representation, which will double the size of the system. Furthermore, distinction between forward and backward whirl disappears using this representation (*11*).

The presence of the damping/gyroscopic matrix, [D], poses a problem for traditional analysis, since the eigen-solution problem uses only two matrices. Converting the problem into the familiar first-order, state-space equation, the general eigenvalue problem becomes

$$-\begin{bmatrix}\mathbf{I} & \mathbf{0}\\ \mathbf{0} & \mathbf{-K}\end{bmatrix}\begin{Bmatrix}\dot{\mathbf{q}}\\ \mathbf{q}\end{Bmatrix}+\begin{bmatrix}\mathbf{0} & \mathbf{I}\\ \mathbf{M} & \mathbf{D}\end{bmatrix}\begin{Bmatrix}\ddot{\mathbf{q}}\\ \dot{\mathbf{q}}\end{Bmatrix}=\begin{Bmatrix}\mathbf{0}\\ \mathbf{0}\end{Bmatrix} \tag{3}$$

or

$$-[\mathbf{A}_1]\{\mathbf{q}'\}+[\mathbf{A}_2]\{\dot{\mathbf{q}}'\}=\{\mathbf{0}\} \tag{4}$$

where

$$[\mathbf{A}_1]=\begin{bmatrix}\mathbf{I} & \mathbf{0}\\ \mathbf{0} & \mathbf{-K}\end{bmatrix},[\mathbf{A}_2]=\begin{bmatrix}\mathbf{0} & \mathbf{I}\\ \mathbf{M} & \mathbf{D}\end{bmatrix},\{\mathbf{q}'\}=\begin{Bmatrix}\dot{\mathbf{q}}\\ \mathbf{q}\end{Bmatrix},\{\dot{\mathbf{q}}'\}=\begin{Bmatrix}\ddot{\mathbf{q}}\\ \dot{\mathbf{q}}\end{Bmatrix} \tag{5}$$

Assuming the displacement and velocity vectors in equation 4 to be of the form:

$$\begin{aligned}\{\mathbf{q}'\}&=\{\mathbf{Q}_o\}e^{\lambda t}\\ \{\dot{\mathbf{q}}'\}&=\lambda\{\mathbf{Q}_o\}e^{\lambda t}\end{aligned} \tag{6}$$

the generalized eigenvalue problem for the state-space formulation becomes

$$\left([\mathbf{A}_1]-\lambda[\mathbf{A}_2]\right)\{\boldsymbol{\phi}_r\}=\{\mathbf{0}\} \tag{7}$$

where (λ) is the complex eigenvalue, and $\{\boldsymbol{\phi}_r\}$ is the corresponding eigenvector. The state-space formulation results in (2N) eigenvalues occurring in complex conjugate pairs, where (N) is the number of DOF of the system.

Returning to equation 2, the system matrices, [M], [K], and [D], are generally not diagonal but have cross-coupling terms throughout. The objective is to determine the mass, stiffness, and damping matrices, respectively as $[M_D]$, $[K_D]$, $[D_D]$, that are diagonal matrices of the transformed equations of motion.

The next step is to calculate the eigenvalues and eigenvectors of the state-space formulation. The results will form two modal matrices, $[\boldsymbol{\Psi}_r]$ and $[\Psi_l]$, whose columns contain the right and left eigenvectors, respectively.

Since the eigenvalues occur in conjugate pairs: $\lambda_i = \alpha \pm j\beta$, the eigenvalues and corresponding eigenvectors can arrange so that the conjugate pairs are separate. From this, two diagonal matrices of dimension ($N \times N$) can be defined that contain the conjugate eigenvalues on the diagonal:

$$\boldsymbol{\Lambda}_1 = \begin{bmatrix} \alpha_1 + \mathrm{j}\beta_1 & 0 & 0 \\ 0 & \ddots & 0 \\ 0 & 0 & \alpha_N + \mathrm{j}\beta_N \end{bmatrix} \tag{8}$$

$$\boldsymbol{\Lambda}_2 = \begin{bmatrix} \alpha_1 - \mathrm{j}\beta_1 & 0 & 0 \\ 0 & \ddots & 0 \\ 0 & 0 & \alpha_N - \mathrm{j}\beta_N \end{bmatrix} \tag{9}$$

If any of the eigenvalues contain purely real roots, the transformation scheme changes somewhat (*9*). However, for brevity, all roots are assumed to be complex.

To ensure the desired results, the right eigenvector must be scaled or normalized. One appropriate scaling results in

$$\boldsymbol{\Psi}_r' = \left[\boldsymbol{\Psi}_r\right]\left[\left[\boldsymbol{\Psi}_l\right]^{\mathrm{T}}\left[\mathbf{A}_2\right]\left[\boldsymbol{\Psi}_r\right]\right]^{-1} \tag{10}$$

such that

$$\begin{aligned} \left[\boldsymbol{\Psi}_l\right]^{\mathrm{T}}\left[\mathbf{A}_1\right]\left[\boldsymbol{\Psi}_r'\right] &= \begin{bmatrix} \boldsymbol{\Lambda}_1 & \mathbf{0} \\ \mathbf{0} & \boldsymbol{\Lambda}_2 \end{bmatrix} = \left[\boldsymbol{\Lambda}\right] \\ \left[\boldsymbol{\Psi}_l\right]^{\mathrm{T}}\left[\mathbf{A}_2\right]\left[\boldsymbol{\Psi}_r'\right] &= \begin{bmatrix} \mathbf{I} & \mathbf{0} \\ \mathbf{0} & \mathbf{I} \end{bmatrix} = \left[\mathbf{I}\right] \end{aligned} \tag{11}$$

Both the left and right eigenvectors are complex, and any further transformations will continue to produce complex numbers. The elimination matrix, [Ξ], is therefore defined to eliminate all complex notation from the transformation.

$$\mathbf{\Xi} = \begin{bmatrix} \frac{1}{\sqrt{2}}\mathbf{I} & \frac{-\mathrm{j}}{\sqrt{2}}\mathbf{I} \\ \frac{1}{\sqrt{2}}\mathbf{I} & \frac{\mathrm{j}}{\sqrt{2}}\mathbf{I} \end{bmatrix} \tag{12}$$

Then

$$\left[\mathbf{\Xi}\right]^{\mathrm{T}}\left[\mathbf{\Psi}_l\right]^{\mathrm{T}}\left[\mathbf{A}_1\right]\left[\mathbf{\Psi}_r'\right]\left[\mathbf{\Xi}\right] = \begin{bmatrix} \mathbf{L}_x & \mathbf{L}_y \\ \mathbf{L}_y & \mathbf{L}_z \end{bmatrix} \tag{13}$$

$$\left[\mathbf{\Xi}\right]^{\mathrm{T}}\left[\mathbf{\Psi}_1\right]^{\mathrm{T}}\left[\mathbf{A}_2\right]\left[\mathbf{\Psi}_r'\right]\left[\mathbf{\Xi}\right] = \begin{bmatrix} \mathbf{I} & \mathbf{0} \\ \mathbf{0} & \mathbf{-I} \end{bmatrix} \tag{14}$$

The matrices $\left[\mathbf{L}_x\right]$, $\left[\mathbf{L}_y\right]$, and $\left[\mathbf{L}_z\right]$ are real and diagonal. They are equal to the following:

$$\begin{aligned} \mathbf{L}_x &= real(\mathbf{\Lambda}_1) \\ \mathbf{L}_y &= imag(\mathbf{\Lambda}_1) \\ \mathbf{L}_z &= -real(\mathbf{\Lambda}_1) = -\mathbf{\Lambda}_x \end{aligned} \tag{15}$$

A diagonal matrix, [**Γ**], is defined.

$$\mathbf{\Gamma}(k,k) = \frac{1}{2}\sinh^{-1}\left(\frac{\mathbf{L}_z(k,k) - \mathbf{L}_x(k,k)}{2\mathbf{L}_y(k,k)}\right) \tag{16}$$

Then the following relationship holds.

$$\begin{bmatrix} \cosh\mathbf{\Gamma} & \sinh\mathbf{\Gamma} \\ \sinh\mathbf{\Gamma} & \cosh\mathbf{\Gamma} \end{bmatrix}\begin{bmatrix} \mathbf{L}_x & \mathbf{L}_y \\ \mathbf{L}_y & \mathbf{L}_z \end{bmatrix}\begin{bmatrix} \cosh\mathbf{\Gamma} & \sinh\mathbf{\Gamma} \\ \sinh\mathbf{\Gamma} & \cosh\mathbf{\Gamma} \end{bmatrix} = \begin{bmatrix} \mathbf{0} & \left[\omega_n\right] \\ \left[\omega_n\right] & \left[2\zeta\omega_n\right] \end{bmatrix} \tag{17}$$

where the matrices $[\omega_n]$ and $[2\zeta\omega_n]$ are diagonal, containing the natural and damped natural frequencies of the system, respectively.

The left and right transformation matrices can now be determined. These are the matrices that diagonalize the state-space matrices [$\mathbf{A}_1$] and [$\mathbf{A}_2$].

$$\mathbf{T}_L = \left[\mathbf{\Psi}_l\right]\left[\mathbf{\Xi}\right]\begin{bmatrix} \cosh\mathbf{\Gamma} & \sinh\mathbf{\Gamma} \\ \sinh\mathbf{\Gamma} & \cosh\mathbf{\Gamma} \end{bmatrix}\begin{bmatrix} \left[\omega_n\right] & \mathbf{0} \\ \mathbf{0} & \mathbf{I} \end{bmatrix} \tag{18}$$

$$\mathbf{T}_R = \left[\boldsymbol{\Psi}_r'\right]\left[\boldsymbol{\Xi}\right]\begin{bmatrix}\cosh\boldsymbol{\Gamma} & \sinh\boldsymbol{\Gamma}\\ \sinh\boldsymbol{\Gamma} & \cosh\boldsymbol{\Gamma}\end{bmatrix}\begin{bmatrix}\left[\omega_n\right] & \mathbf{0}\\ \mathbf{0} & \mathbf{I}\end{bmatrix} \tag{19}$$

Transforming, the diagonalized results become

$$\left[\mathbf{T}_L\right]^{\mathrm{T}}\left[\mathbf{A}_1\right]\left[\mathbf{T}_R\right] = \left[\mathbf{B}_1\right] = \begin{bmatrix}\mathbf{0} & \mathbf{K}_D\\ \mathbf{K}_D & \mathbf{D}_D\end{bmatrix} \tag{20}$$

$$\left[\mathbf{T}_L\right]^{\mathrm{T}}\left[\mathbf{A}_2\right]\left[\mathbf{T}_R\right] = \left[\mathbf{B}_2\right] = \begin{bmatrix}\mathbf{K}_D & \mathbf{0}\\ \mathbf{0} & -\mathbf{M}_D\end{bmatrix} \tag{21}$$

This transformation methodology will result in (2*N*) de-coupled linearly independent equations. The usual relationships achieved through modal analysis apply here as well, namely

$$\begin{aligned}\mathbf{M}_D &= \mathbf{I}\\ \mathbf{D}_D &= [2\zeta\omega_n]\\ \mathbf{K}_D &= [\omega_n^2]\end{aligned} \tag{22}$$

If carried through from start to finish, the process produces results consistent with the following simplification (*12*).

$$\begin{aligned}\lambda_{i1} &= \alpha + \mathrm{j}\beta\\ \lambda_{i2} &= \alpha - \mathrm{j}\beta\\ d_i &= -\left(\lambda_{i1} + \lambda_{i2}\right) = -2\alpha_i\\ k_i &= \frac{\left(\lambda_{i2} + \lambda_{i1}\right)^2 - \left(\lambda_{i2} - \lambda_{i1}\right)^2}{4} = \alpha_i^2 + \beta_i^2\\ m_i &= 1\end{aligned} \tag{23}$$

where $i = 1 \ldots N$

From modal analysis, the transformed coordinates, {**v**}, are principal coordinates. The transformation to the physical coordinate system is

$$\begin{Bmatrix}\dot{\mathbf{q}}\\ \mathbf{q}\end{Bmatrix} = \left[\mathbf{T}_R\right]\begin{Bmatrix}\mathbf{v}\\ \mathbf{u}\end{Bmatrix} \tag{24}$$

In the equation above, the term, {**u**} is not necessarily the time derivative of the general coordinate, {**v**}, except when the system is in free vibration (*9*). Also, the vector order of the principal coordinate and its "derivative" are reversed compared to the physical coordinates.

2.2 Transformation Simplification

The full procedure outlined in the previous section is rigorous and lengthy. However, a simplified transformation is available using equation 23 and similarity transformation relationships. From the definition of a similarity transformation,

$$\left[\boldsymbol{\Psi}_l\right]^{\mathrm{T}}\left[\mathbf{A}_1\right]\left[\boldsymbol{\Psi}'_r\right]=\left[\boldsymbol{\Lambda}\right]=\left[\boldsymbol{\Phi}_l\right]^{\mathrm{T}}\left[\mathbf{B}_1\right]\left[\boldsymbol{\Phi}'_r\right] \tag{25}$$

$$\left[\boldsymbol{\Psi}_l\right]^{\mathrm{T}}\left[\mathbf{A}_2\right]\left[\boldsymbol{\Psi}'_r\right]=\left[\mathbf{I}\right]=\left[\boldsymbol{\Phi}_l\right]^{\mathrm{T}}\left[\mathbf{B}_2\right]\left[\boldsymbol{\Phi}'_r\right] \tag{26}$$

where $[\boldsymbol{\Phi}_r]$ and $[\boldsymbol{\Phi}_l]$ are the modal matrices of the reduced system. Using linear algebra, the transformation matrices $[\mathbf{T}_L]$ and $[\mathbf{T}_R]$ can be written as (*12*)

$$\left[\mathbf{T}_L\right]=\left[\boldsymbol{\Psi}_l\right]\left[\boldsymbol{\Phi}_l\right]^{-1} \tag{27}$$

$$\left[\mathbf{T}_R\right]=\left[\boldsymbol{\Psi}'_r\right]\left[\boldsymbol{\Phi}'_r\right]^{-1} \tag{28}$$

Using these relationships, the simplified transformation procedure is as follows:

1. Given matrices $[\mathbf{A}_1]$ and $[\mathbf{A}_2]$, solve the eigenvalue problem. Arrange the eigenvalues in matrices $[\boldsymbol{\Lambda}_1]$ and $[\boldsymbol{\Lambda}_2]$. Assemble the left, $[\boldsymbol{\Psi}_l]$, and right normalized, $\left[\boldsymbol{\Psi}'_r\right]$, eigenvector matrices, corresponding to $[\boldsymbol{\Lambda}_1]$ and $[\boldsymbol{\Lambda}_2]$.
2. Using equation 23, calculate the diagonal values of $[\mathbf{M}_D]$, $[\mathbf{K}_D]$, $[\mathbf{D}_D]$. Substitute into equations 20 and 21 for $[\mathbf{B}_1]$ and $[\mathbf{B}_2]$, respectively.
3. Determine the left, $[\boldsymbol{\Phi}_l]$, and right, $\left[\boldsymbol{\Phi}'_r\right]$, normalized eigenvector matrices of the modal system, $[\mathbf{B}_1]$ and $[\mathbf{B}_2]$.
4. Substitute into equations 27 and 28 to solve for $[\mathbf{T}_L]$ and $[\mathbf{T}_R]$, respectively.

In order to ensure more precise results, it is possible to further refine the transformation by calculating the left eigenvector matrix, $[\boldsymbol{\Psi}_l]$, using either equation 20 or 21, rather than using the originally determined left eigenvector matrix. The results are then substituted into equations 27 and 28.

3. Modal Synthesis

3.1 Theory

In modal synthesis, the analysis begins with the substructures. The equations of motion for each substructure are

$$\left[\mathbf{M}_i\right]\left\{\ddot{\mathbf{q}}_i\right\}+\left[\mathbf{D}_i\right]\left\{\dot{\mathbf{q}}_i\right\}+\left[\mathbf{K}_i\right]\left\{\mathbf{q}_i\right\}=\left\{\mathbf{F}\left(t\right)_i\right\} \tag{29}$$

where the subscript, (i), represents the i^{th} substructure. The substructure eigenvalue problem solution follows the state-space methodology introduced in equation 3.

$$-\begin{bmatrix}\mathbf{I} & \mathbf{0}\\ \mathbf{0} & -\mathbf{K}\end{bmatrix}_i\begin{Bmatrix}\dot{\mathbf{q}}\\ \mathbf{q}\end{Bmatrix}+\begin{bmatrix}\mathbf{0} & \mathbf{I}\\ \mathbf{M} & \mathbf{D}\end{bmatrix}_i\begin{Bmatrix}\ddot{\mathbf{q}}\\ \dot{\mathbf{q}}\end{Bmatrix}=\begin{Bmatrix}\mathbf{0}\\ \mathbf{F(t)}\end{Bmatrix}_i \tag{30}$$

Once the substructure analysis is complete, the global, uncoupled system is constructed. However, unlike some other modal synthesis works (*13*), the entire state-space formulation of equation 30 becomes part of the global model. The dimensions of the global state-space formulation are $[(2N_1 + \ldots + 2N_m) \times (2N_1 + \ldots + 2N_m)]$.

$$-\begin{bmatrix}\begin{bmatrix}\mathbf{I} & \mathbf{0}\\ \mathbf{0} & -\mathbf{K}\end{bmatrix}_1 & & \mathbf{0}\\ & \ddots & \\ \mathbf{0} & & \begin{bmatrix}\mathbf{I} & \mathbf{0}\\ \mathbf{0} & -\mathbf{K}\end{bmatrix}_m\end{bmatrix}\begin{Bmatrix}\begin{Bmatrix}\dot{\mathbf{q}}\\ \mathbf{q}\end{Bmatrix}_1\\ \vdots\\ \begin{Bmatrix}\dot{\mathbf{q}}\\ \mathbf{q}\end{Bmatrix}_m\end{Bmatrix}+\begin{bmatrix}\begin{bmatrix}\mathbf{0} & \mathbf{I}\\ \mathbf{M} & \mathbf{D}\end{bmatrix}_1 & & \mathbf{0}\\ & \ddots & \\ \mathbf{0} & & \begin{bmatrix}\mathbf{0} & \mathbf{I}\\ \mathbf{M} & \mathbf{D}\end{bmatrix}_m\end{bmatrix}\begin{Bmatrix}\begin{Bmatrix}\ddot{\mathbf{q}}\\ \dot{\mathbf{q}}\end{Bmatrix}_1\\ \vdots\\ \begin{Bmatrix}\ddot{\mathbf{q}}\\ \dot{\mathbf{q}}\end{Bmatrix}_m\end{Bmatrix}=\begin{Bmatrix}\begin{Bmatrix}\mathbf{0}\\ \mathbf{F(t)}\end{Bmatrix}_1\\ \vdots\\ \begin{Bmatrix}\mathbf{0}\\ \mathbf{F(t)}\end{Bmatrix}_m\end{Bmatrix} \tag{31}$$

or in simpler notation

$$\begin{bmatrix}\left[\mathbf{A}_1\right]_1 & & \mathbf{0}\\ & \ddots & \\ \mathbf{0} & & \left[\mathbf{A}_1\right]_m\end{bmatrix}\begin{Bmatrix}\left\{\mathbf{q}'\right\}_1\\ \vdots\\ \left\{\mathbf{q}'\right\}_m\end{Bmatrix}+\begin{bmatrix}\left[\mathbf{A}_2\right]_1 & & \mathbf{0}\\ & \ddots & \\ \mathbf{0} & & \left[\mathbf{A}_2\right]_m\end{bmatrix}\begin{Bmatrix}\left\{\dot{\mathbf{q}}'\right\}_1\\ \vdots\\ \left\{\dot{\mathbf{q}}'\right\}_m\end{Bmatrix}=\begin{Bmatrix}\left\{\mathbf{F(t)}\right\}_1\\ \vdots\\ \left\{\mathbf{F(t)}\right\}_m\end{Bmatrix} \tag{32}$$

where (m) is the number of substructures in the system.

For simplicity, equation 32 can be rewritten as

$$\left[\mathbf{A}_1^*\right]\left\{\mathbf{q}^*\right\}+\left[\mathbf{A}_2^*\right]\left\{\dot{\mathbf{q}}^*\right\}=\left\{\mathbf{F(t)}^*\right\} \tag{33}$$

where the asterisk symbolizes the global system of individual substructures. Note that the substructure coupling has not been introduced yet.

Returning to the fundamental concept of modal analysis, the system equations of motion are transformed into principal coordinates. The global transformation matrices are composed of the substructure transformation matrices of equations 27 and 28, respectively.

$$\left[\mathbf{T}_L^*\right]^{\mathrm{T}}\left[\mathbf{A}_1^*\right]\left[\mathbf{T}_R^*\right]\left\{\mathbf{v}^*\right\}+\left[\mathbf{T}_L^*\right]^{\mathrm{T}}\left[\mathbf{A}_2^*\right]\left[\mathbf{T}_R^*\right]\left\{\dot{\mathbf{v}}^*\right\}=\left[\mathbf{T}_L^*\right]^{\mathrm{T}}\left\{\mathbf{F}(\mathbf{t})^*\right\} \tag{34}$$

where

$$\left[\mathbf{T}_L^*\right]=\begin{bmatrix}\left[\mathbf{T}_L\right]_1 & & \mathbf{0}\\ & \ddots & \\ \mathbf{0} & & \left[\mathbf{T}_L\right]_m\end{bmatrix},\left[\mathbf{T}_R^*\right]=\begin{bmatrix}\left[\mathbf{T}_R\right]_1 & & \mathbf{0}\\ & \ddots & \\ \mathbf{0} & & \left[\mathbf{T}_R\right]_m\end{bmatrix} \tag{35}$$

Equation 34 simplifies to

$$\left[\mathbf{B}_1^*\right]\left\{\mathbf{v}^*\right\}-\left[\mathbf{B}_2^*\right]\left\{\dot{\mathbf{v}}^*\right\}=\left[\mathbf{T}_L^*\right]^{\mathrm{T}}\left\{\mathbf{F}(\mathbf{t})^*\right\} \tag{36}$$

or in long form,

$$\begin{bmatrix}\begin{bmatrix}\mathbf{0} & \mathbf{K}_D\\ \mathbf{K}_D & \mathbf{D}_D\end{bmatrix}_1 & & \mathbf{0}\\ & \ddots & \\ \mathbf{0} & & \begin{bmatrix}\mathbf{0} & \mathbf{K}_D\\ \mathbf{K}_D & \mathbf{D}_D\end{bmatrix}_m\end{bmatrix}\begin{Bmatrix}\begin{Bmatrix}\mathbf{u}\\ \mathbf{v}\end{Bmatrix}_1\\ \vdots\\ \begin{Bmatrix}\mathbf{u}\\ \mathbf{v}\end{Bmatrix}_m\end{Bmatrix}-\begin{bmatrix}\begin{bmatrix}\mathbf{K}_D & \mathbf{0}\\ \mathbf{0} & \text{-}\mathbf{M}\end{bmatrix}_1 & & \mathbf{0}\\ & \ddots & \\ \mathbf{0} & & \begin{bmatrix}\mathbf{K}_D & \mathbf{0}\\ \mathbf{0} & \text{-}\mathbf{M}\end{bmatrix}_m\end{bmatrix}\begin{Bmatrix}\begin{Bmatrix}\dot{\mathbf{u}}\\ \dot{\mathbf{v}}\end{Bmatrix}_1\\ \vdots\\ \begin{Bmatrix}\dot{\mathbf{u}}\\ \dot{\mathbf{v}}\end{Bmatrix}_m\end{Bmatrix}=\left[\mathbf{T}_L^*\right]^{\mathrm{T}}\begin{Bmatrix}\begin{Bmatrix}\mathbf{0}\\ \mathbf{F}(\mathbf{t})\end{Bmatrix}_1\\ \vdots\\ \begin{Bmatrix}\mathbf{0}\\ \mathbf{F}(\mathbf{t})\end{Bmatrix}_m\end{Bmatrix} \tag{37}$$

Note that the global equation containing the (*m*) systems is still uncoupled.

The coupling occurs as a result of the gear mesh. The mesh stiffness is the coupling agent. However, this treatment is general enough to apply to other types of couplings with only minor changes to the methodology.

The mesh matrix, [$\mathbf{K}_{mesh}$], breaks into quadrants as shown below. A methodology for determining the components of the mesh matrix for spur or helical gears can be found in (*14*).

$$\left[\mathbf{K}_{mesh}\right]=\begin{bmatrix}\left[\mathbf{K}_{mesh}\right]_{ii} & \left[\mathbf{K}_{mesh}\right]_{ij}\\ \left[\mathbf{K}_{mesh}\right]_{ji} & \left[\mathbf{K}_{mesh}\right]_{jj}\end{bmatrix} \tag{38}$$

For a two-shaft system, the coupling becomes

$$\left[\mathbf{A}_1^*\right]_{sys} = \begin{bmatrix} \begin{bmatrix} \mathbf{I} & \mathbf{0} \\ \mathbf{0} & -\mathbf{K} \end{bmatrix}_1 & \mathbf{0} \\ \mathbf{0} & \begin{bmatrix} \mathbf{I} & \mathbf{0} \\ \mathbf{0} & -\mathbf{K} \end{bmatrix}_2 \end{bmatrix} + \begin{bmatrix} \begin{bmatrix} \mathbf{0} & \mathbf{0} \\ \mathbf{0} & -\left[\mathbf{K}_{mesh}\right]_{i,i} \end{bmatrix} & \begin{bmatrix} \mathbf{0} & \mathbf{0} \\ \mathbf{0} & -\left[\mathbf{K}_{mesh}\right]_{i,j} \end{bmatrix} \\ \begin{bmatrix} \mathbf{0} & \mathbf{0} \\ \mathbf{0} & -\left[\mathbf{K}_{mesh}\right]_{j,i} \end{bmatrix} & \begin{bmatrix} \mathbf{0} & \mathbf{0} \\ \mathbf{0} & -\left[\mathbf{K}_{mesh}\right]_{j,j} \end{bmatrix} \end{bmatrix} \tag{39}$$

or

$$\left[\mathbf{A}_1^*\right]_{sys} = \left[\mathbf{A}_1^*\right] + \left[\mathbf{A}_1^*\right]_{mesh} \tag{40}$$

Using the same transformation on the second term in equation 39 results in the transformed coupling matrix, [$\mathbf{K}_{Dm}$].

$$\left[\mathbf{B}_1^*\right]_{mesh} = \left[\mathbf{T}_L^*\right]^{\mathrm{T}} \begin{bmatrix} \begin{bmatrix} \mathbf{0} & \mathbf{0} \\ \mathbf{0} & -\left[\mathbf{K}_{mesh}\right]_{i,i} \end{bmatrix} & \begin{bmatrix} \mathbf{0} & \mathbf{0} \\ \mathbf{0} & -\left[\mathbf{K}_{mesh}\right]_{i,j} \end{bmatrix} \\ \begin{bmatrix} \mathbf{0} & \mathbf{0} \\ \mathbf{0} & -\left[\mathbf{K}_{mesh}\right]_{j,i} \end{bmatrix} & \begin{bmatrix} \mathbf{0} & \mathbf{0} \\ \mathbf{0} & -\left[\mathbf{K}_{mesh}\right]_{j,j} \end{bmatrix} \end{bmatrix} \left[\mathbf{T}_R^*\right] = \begin{bmatrix} \begin{bmatrix} \mathbf{0} & \mathbf{0} \\ \mathbf{0} & \left[\mathbf{K}_{Dm}\right]_{i,i} \end{bmatrix} & \begin{bmatrix} \mathbf{0} & \mathbf{0} \\ \mathbf{0} & \left[\mathbf{K}_{Dm}\right]_{i,j} \end{bmatrix} \\ \begin{bmatrix} \mathbf{0} & \mathbf{0} \\ \mathbf{0} & \left[\mathbf{K}_{Dm}\right]_{j,i} \end{bmatrix} & \begin{bmatrix} \mathbf{0} & \mathbf{0} \\ \mathbf{0} & \left[\mathbf{K}_{Dm}\right]_{j,j} \end{bmatrix} \end{bmatrix} \tag{41}$$

Note that since this is a coupling matrix, it is not necessarily diagonal. Thus the coupled system modal matrix, $\left[\mathbf{B}_1^*\right]_{sys}$, is

$$\left[\mathbf{B}_1^*\right]_{sys} = \left[\mathbf{B}_1^*\right] + \left[\mathbf{B}_1^*\right]_{mesh} \tag{42}$$

In this formulation, it is assumed that no damping occurs in the gear mesh. Consequently, the gear mesh does not affect the modal system matrix, $\left[\mathbf{B}_2^*\right]$ from equation 36. It requires no modification:

$$\left[\mathbf{B}_2^*\right]_{sys} = \left[\mathbf{B}_2^*\right] \tag{43}$$

Equation 36 then becomes

$$\left[\mathbf{B}_1^*\right]_{sys} \left\{\mathbf{v}^*\right\}_{sys} - \left[\mathbf{B}_2^*\right]_{sys} \left\{\dot{\mathbf{v}}^*\right\}_{sys} = \left[\mathbf{T}_L^*\right]^{\mathrm{T}} \left\{\mathbf{F(t)}^*\right\}_{sys} \tag{44}$$

The general eigenvalue problem of equation 44 yields the same results as the original problem of equation 3.

As with the transformation sequence, the steps for reduction are as follows:

1. Define a variable, (P), that represents the number of DOF of the reduced system model. The only caveat is that the selection of (P) must be divisible by 2. The resulting state space matrices $\left[\mathbf{B}_1^*\right]_{sys}$ and $\left[\mathbf{B}_2^*\right]_{sys}$ will have dimensions ($2P \times 2P$). This requires (P) to be smaller than the lowest subsystem DOF.

2. Reduce the size of modal matrices, $\left[\mathbf{T}_L^*\right]$ and $\left[\mathbf{T}_R^*\right]$, to dimensions ($2N_1 + \ldots + 2N_m \times 2P$) by discarding the unnecessary columns of the modal matrices. Since this is a state-space formulation, the columns associated with each of the ($2m$) vector components (i.e., $\left\{\dot{\mathbf{q}}_1\right\}_{N_1\times 1}, \left\{\mathbf{q}_1\right\}_{N_1\times 1}, \left\{\dot{\mathbf{q}}_2\right\}_{N_2\times 1}, \left\{\mathbf{q}_2\right\}_{N_2\times 1} \cdots \left\{\dot{\mathbf{q}}_m\right\}_{N_3\times 1}, \left\{\mathbf{q}_m\right\}_{N_3\times 1}$) must undergo an equal reduction. The size of the reduced system is ($2P \times 2P$). The selection matrices from $\left[\mathbf{T}_L^*\right]$ and $\left[\mathbf{T}_R^*\right]$ will result in an equal number of modes selected from the original eigen matrices associated with each vector component. The reduced transformation matrices, $\left[\mathbf{T}_L^*\right]$ and $\left[\mathbf{T}_R^*\right]$, will thus have dimensions ($2N_1 + \ldots + 2N_m \times 2P$).

3. Transform the system matrices, $\left[\mathbf{A}_1^*\right]_{sys}$ and $\left[\mathbf{A}_2^*\right]_{sys}$, using the reduced transformation matrices, $\left[\mathbf{T}_L^*\right]$ and $\left[\mathbf{T}_R^*\right]$. This results in the reduced diagonal matrices of equation 45.

$$\begin{aligned}\left[\mathbf{T}_L^*\right]^{\mathrm{T}}_{\left(2P\times 2N_1+\cdots+2N_m\right)}\left[\mathbf{A}_1^*\right]_{sys\left(2N_1+\cdots+2N_m\times 2N_1+\cdots+2N_m\right)}\left[\mathbf{T}_R^*\right]_{\left(2N_1+\cdots+2N_m\times 2P\right)} &= \left[\mathbf{B}_1^*\right]_{sys\left(2P\times 2P\right)}\\ \left[\mathbf{T}_L^*\right]^{\mathrm{T}}_{\left(2P\times 2N_1+\cdots+2N_m\right)}\left[\mathbf{A}_2^*\right]_{sys\left(2N_1+\cdots+2N_m\times 2N_1+\cdots+2N_m\right)}\left[\mathbf{T}_R^*\right]_{\left(2N_1+\cdots+2N_m\times 2P\right)} &= \left[\mathbf{B}_2^*\right]_{sys\left(2P\times 2P\right)}\end{aligned} \tag{45}$$

4. Solve the eigenvalue problem of the reduced state-space matrices, $\left[\mathbf{B}_1^*\right]_{sys\left(2P\times 2P\right)}$ and $\left[\mathbf{B}_2^*\right]_{sys\left(2P\times 2P\right)}$. The eigenvalues will result in (P) complex conjugate pairs, which represent the first (P) frequencies of the system. They will have the same or very near the same value as the corresponding frequencies of the full system model.

3.2 Speed-Sweep Vibration Response

The determination of the vibration response is possible using the principal coordinates as well. Returning to equation 44, one can assume a harmonic response to the forcing function, $\{\mathbf{F(t)^*}\}_{sys}$:

$$\left\{\mathbf{V}^*\right\}_{sys} = \left\{\mathbf{V}^*\right\}\mathrm{e}^{\mathrm{j}\omega t} \tag{46}$$

such that the equations of motion become

$$\left[\mathbf{B}_1^*\right]_{sys}\left\{\mathbf{V}^*\right\}_{sys} - \mathrm{j}\omega\left[\mathbf{B}_2^*\right]_{sys}\left\{\mathbf{V}^*\right\}_{sys} = \left[\mathbf{T}_L^*\right]^{\mathrm{T}}\left\{\mathbf{F}_0^*\right\}_{sys} \tag{47}$$

The displacements in modal coordinates are

$$\left\{\mathbf{V}^*\right\}_{sys} = \left[\left[\mathbf{B}_1^*\right]_{sys} - \mathrm{j}\omega\left[\mathbf{B}_2^*\right]_{sys}\right]^{-1}\left[\mathbf{T}_L^*\right]^{\mathrm{T}}\left\{\mathbf{F}_0^*\right\}_{sys} \tag{48}$$

Converting back to physical coordinates yields the following expression:

$$\left\{\mathbf{Q}^*\right\}_{sys} = \left[\mathbf{T}_R^*\right]\left[\left[\mathbf{B}_1^*\right]_{sys} - \mathrm{j}\omega\left[\mathbf{B}_2^*\right]_{sys}\right]^{-1}\left[\mathbf{T}_L^*\right]^{\mathrm{T}}\left\{\mathbf{F}_0^*\right\}_{sys} \tag{49}$$

where $\{\mathbf{Q^*}\}_{sys}$ is the vector containing the amplitudes of the response. Substituting the operational speeds, (Ω), into equation 49 will yield speed sweep vibration responses, as shown later in figures 3 and 4.

Gyroscopic effects play a unique role in speed-sweep response. The modal transformation matrices are determined by calculating the eigenvectors of the system. The matrix, [**D**], contains the system gyroscopics, which is a function of rotational speed. Hence, the eigenvectors themselves are a function of rotational speed, and the transformation matrices themselves change with rotational speed. Consequently, for a full, modal speed-sweep analysis, the transformation matrices must be calculated at each speed interval within the desired range. Additionally, the frequency response can be calculated by fixing the operational speed in the [**D**] matrix and varying the frequency (ω) in equation 49.

3.3 Time Domain Response

If desired, it is also possible to determine the time domain forced response using equation 49. The time domain response acts at a single frequency. The shaft operating speed is simply substituted into equation 49 to solve for the amplitude vector, $\{\mathbf{Q^*}\}_{eye}$. The time domain response is simply the periodic function:

$$\left\{\mathbf{q}^*\right\}_{sys} = \left\{\mathbf{Q}^*\right\}_{sys} \mathrm{e}^{\mathrm{j}wt} \tag{50}$$

4. Application: Geared System with Damping

4.1 Overview

The application for preliminary validation of this methodology is a basic model of a spur gear shaft pair similar to the one found in figure 1. Selected because of the ready availability of the system parameters, it appears a number of times in the literature (*15, 16*). The system consists of two identical spur gears resting at the midpoint of identical shafts, each connected to the gearbox by a pair of rolling-element bearings. Since the two substructures are the same, the reduction in the complexity of equation 30 is significant. All substructure matrix components are identical for each substructure. Table 1 provides the parameters of the two-shaft system.

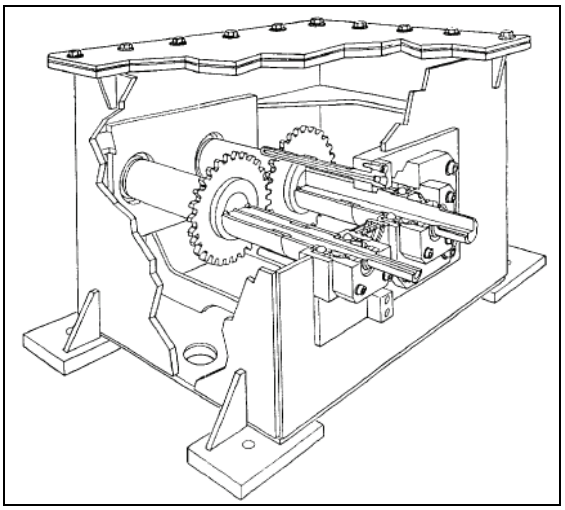

Figure 1. Spur gear test stand (*15*).

Table 1. Spur gear application system parameters.

Material Parameters	
Young's Modulus (N/m^2)	2.03E11
Shear Modulus (N/m^2)	8.0E10
Poission's Ratio	0.3
Density (kg/m^3)	7750
Shaft Parameters	
Length (m)	0.254
Mass (kg)	1.96
Rigidity ($N\text{-}m^2$)	18576
Outer Diameter (m)	0.037
Inner Diameter (m)	0.01
Gear Parameters	
Mass (kg)	1.84
Moment of Inertia ($kg\text{-}m^2$)	1.8E-3
Polar Moment of Inertia ($kg\text{-}m^2$)	3.6E-3
Diameter (m)	0.089
Pressure Angle (deg)	20
Helical Angle (deg)	0.0
Average Mesh Stiffness (N/m)	1.0E8
Bearing Parameters	
k_{xx}, k_{yy} ($N\text{-}s/m$)	1.0E9
c_{xx} ($N\text{-}s/m$)	500
c_{yy} ($N\text{-}s/m$)	700

The gear mesh is, in actuality, a periodic (non-linear) stiffness due to the alternating number of teeth in contact throughout the mesh cycle. This closed-form solution linearizes the equations of motion by assuming an average mesh stiffness value (table 1). Otherwise, for non-linear treatment, numerical integration techniques become necessary (*4*)

The full finite element system model calculates the eigen solution of the system and the frequency response to a harmonic forcing function. Each shaft consists of 126 DOF, or 252 for the entire system. Since the state-space formulation doubles the size of the model, the total number of DOF is 504. The software used in this formulation was MATLAB®.

Prior to any modal reduction, the validity of the system model was accessed through a comparison of natural frequencies at low speed and low damping to those previously published in the literature (*16, 17*). As depicted in figure 2, the model provides results consistent with previous experiments. The *x*-axis of figure 2 contains no values. It is a set of bins that categorizes the like frequencies of the three sets of data.

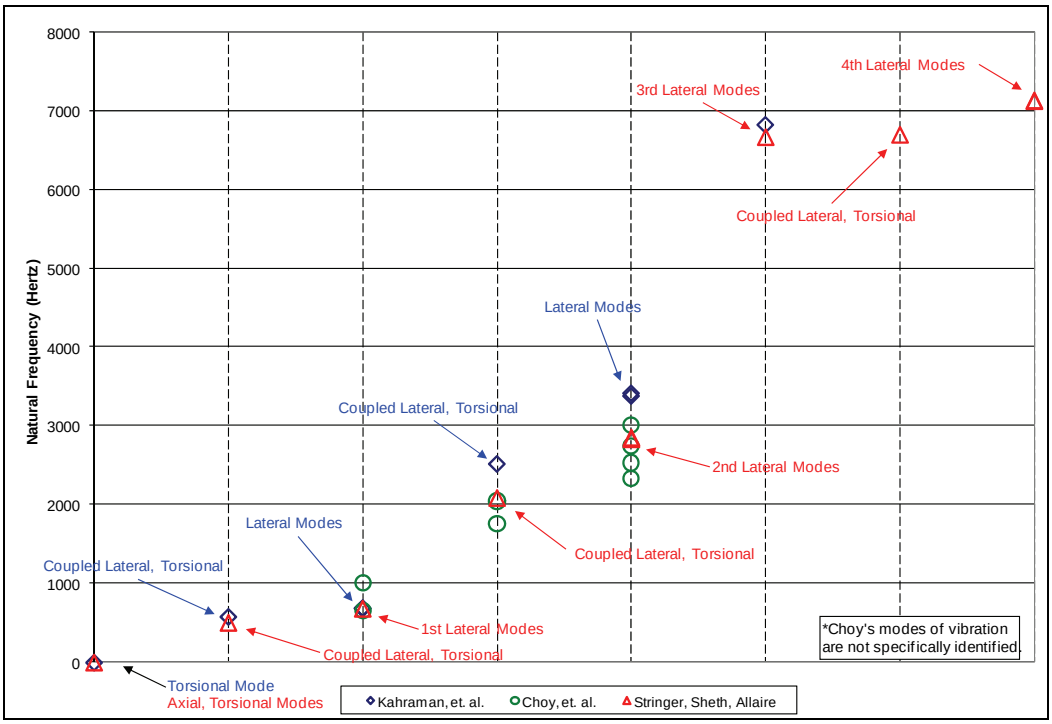

Figure 2. Comparison with previous results (*16,17*).

4.2 Modal Reduction Comparisons

Since modal analysis is an approximation, it requires further validation through comparison with the full system model results. The first validation compares the eigenvalues of the system model with those of the reduced model. Tables 2 and 3 provide the results of reductions to (P) = 30 and 20 DOF, respectively. The rotational speed (Ω) for this analysis is 1000 rpm or 16.67 Hz. For brevity, only the first 10 frequencies are provided.

Table 2. Modal analysis eigenvalue comparison (P=30).

	Modal Synthesis (*Hz*)	**Full FEA (*Hz*)**	**Difference (%)**
1	504.647	504.635	0.00%
2	684.261	684.260	0.00%
3	684.279	684.279	0.00%
4	684.296	684.297	0.00%
5	2091.562	2090.630	0.04%
6	2837.572	2837.560	0.00%
7	2837.572	2837.560	0.00%
8	2858.979	2858.969	0.00%
9	2858.979	2858.969	0.00%
10	6677.140	6676.739	0.01%

Table 3. Modal synthesis eigenvalue comparison (P=20).

	Modal Synthesis (*Hz*)	**Full FEA (*Hz*)**	**Difference (%)**
1	504.65204	504.635	0.00%
2	684.261	684.260	0.00%
3	684.279	684.279	0.00%
4	684.296	684.297	0.00%
5	2091.950	2090.630	0.06%
6	2837.572	2837.560	0.00%
7	2837.572	2837.560	0.00%
8	2858.979	2858.969	0.00%
9	2858.979	2858.969	0.00%
10	6677.140	6676.739	0.01%

These results clearly show the levels of accuracy attainable by modal synthesis. Furthermore, the modal simplifications also produce substantial reductions in the amount of computing time required compared to the full system model: 62% and 63%, respectively.

The second validation method occurs by comparing the reduced system's speed-sweep responses to excitation. The responses of two harmonic forcing functions are presented. The first is the gear-meshing frequency. The gear-mesh frequency is a result of the clatter between gears as the gear teeth come in and out of contact with each other and the nonlinear loading of the gear mesh. It is present in all gears and for spur and helical gears, it is defined as the number of gear teeth multiplied by the shaft rotational seed. The key impact of the gear-mesh frequency is that it excites higher modes of vibration at lower rotational speeds.

The second forcing function models a mass imbalance in one of the gears. A finite imbalance exists in all rotating systems and is a function of the rotational speed squared, $(\Omega)^2$. Figures 3 and 4 provide the speed-sweep responses for the gear-mesh frequency and mass imbalance excitations, respectively, using a speed step, ($\Delta\Omega$), of 50 Hz.

The response curves represent the lateral displacement of each shaft at its midpoint. Three curves are plotted for each shaft, providing the results of (1) the full finite element model – "Full FEA," (2) the full modal reduction – "Modal Synthesis," and (3) the modal reduction using a fixed operating speed – Modal Fixed Gyro." The Modal Synthesis scenario recalculates the transformation matrices for each rotational speed interval. The Modal Fixed Gyro scenario calculates the matrices only once for a single value within the desired speed range in order to reduce the number of burdensome eigenvector calculations. It then uses these matrices for all responses within the operating range, 0-5000 Hz. Figures 3 and 4 show that for this system, the difference between these two approaches is negligible.

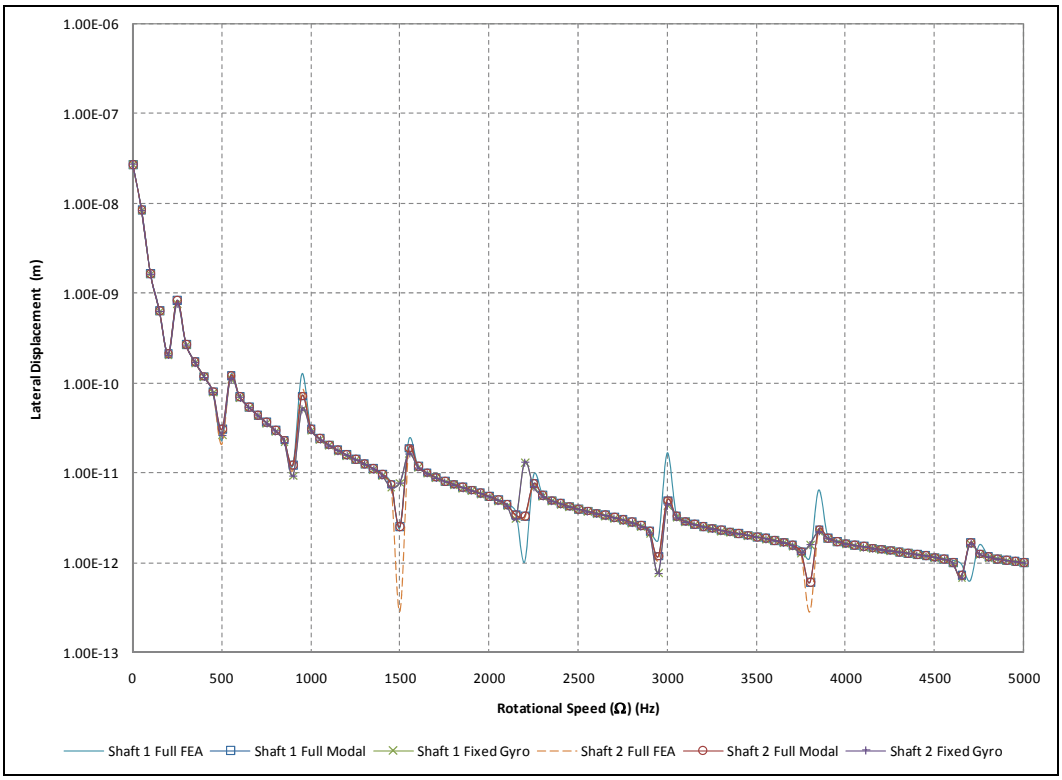

Figure 3. Gear-mesh frequency response comparison (0-5000 Hz).

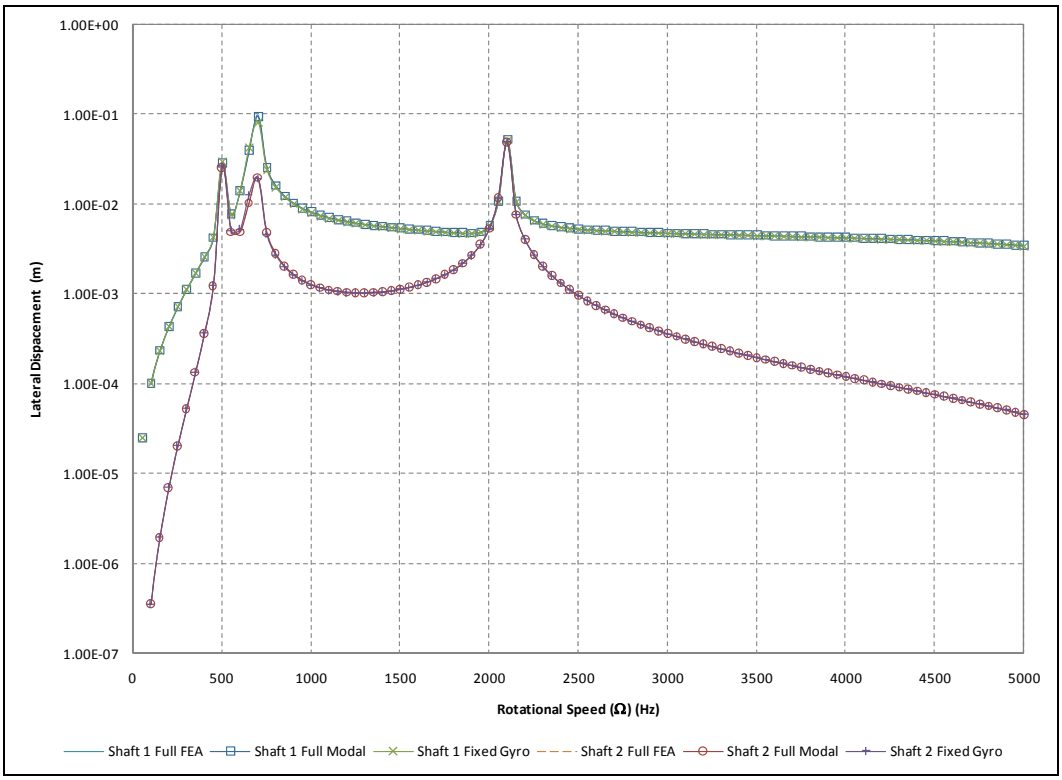

Figure 4. Imbalance response comparison (0-5000 Hz).

If necessary, the time domain response can also be determined. This might be desirable if the shape of one of the shaft orbits is important. Figure 5 shows four views of the combined horizontal and vertical vibrations for a single shaft. The top-left plot simply shows the circular motion of the vibration over time. The top-right chart shows the shape of the orbit. The bottom two charts simply show the sinusoidal motion of the vibration in the horizontal (left) and vertical (right) planes of motion.

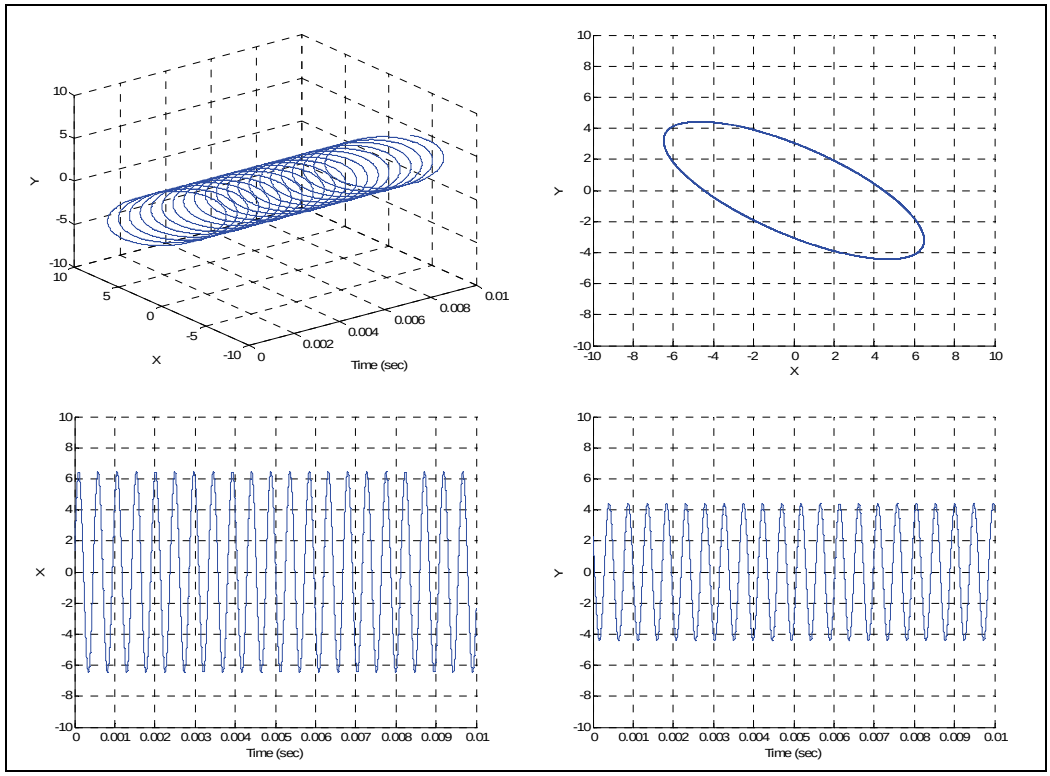

Figure 5. Time response of damped gear shaft due to excitation near resonance.

5. Discussion – Modal Synthesis Practicality in Geared System Application

For all its accuracy, this experiment does raise some questions regarding the utility of such procedure in terms of practicality and efficiency. These questions fall into two categories: limitations on modal reduction and the impact of the gyroscopic effect.

5.1 Limitations on Modal Reduction

Once again, the modal synthesis procedure can produce a significant modal reduction without loss of accuracy. However, in the speed-sweep response, the gear-mesh forcing function will limit the amount of reduction available. At lower speeds, the gear-mesh frequency will excite higher modes of vibration. Consequently, for the modal synthesis transformation to capture these higher modes, they must be included in the modal reduction. An example is presented in figure 6.

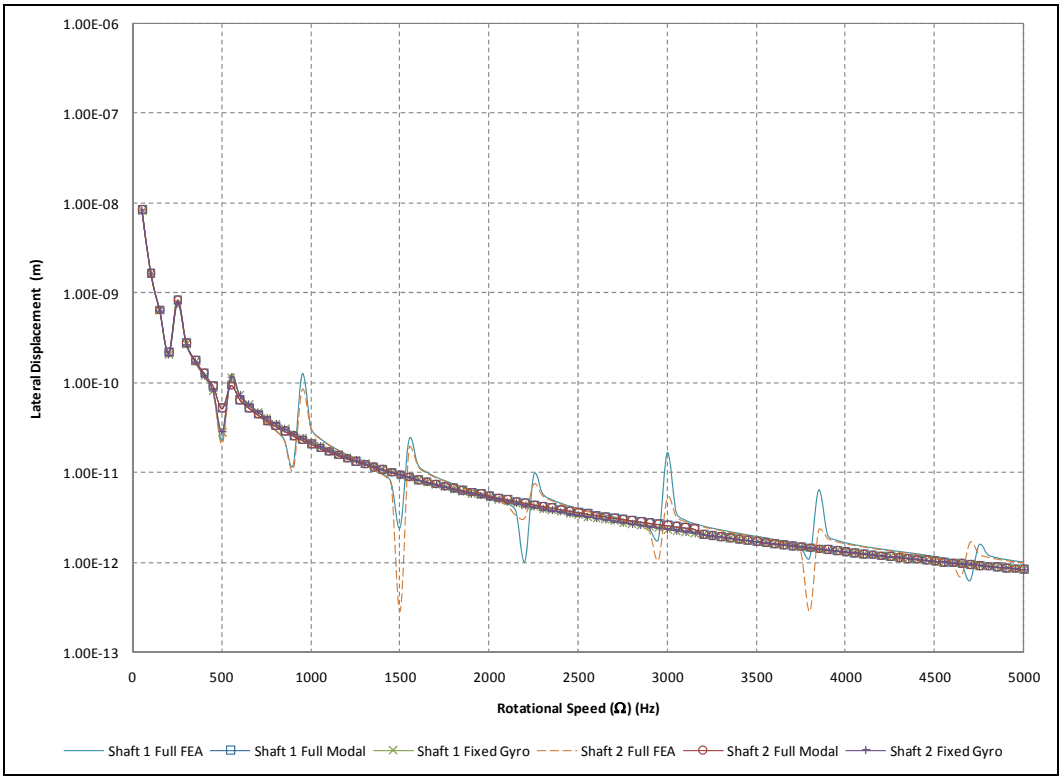

Figure 6. Gear-mesh frequency limitations on modal reduction.

The total number of DOF in the geared, two-shaft model is 252. This increases to 504 DOF in the state-space. Figure 6 illustrates a modal reduction to 30 DOF (60 DOF in the state-space) in terms of the gear-mesh forcing function response. The reduced model has failed to accurately portray all resonance peaks within the operating range, 0-5000 Hz. To capture the remaining peaks, the modal DOF must increase to account for excitation of the higher modes. For the application system, the required number of degrees of freedom to produce an accurate response is 168, or in the state-space, 336. Thus, an intended 88% DOF reduction will result in a reduction of only 33% if the gear-meshing frequency excitation is important.

The implication for geared system analysis is that there must be some *a priori* knowledge as to the number of higher modes excited within the desired operating speed range. An increase in the number of gear teeth or the operating range itself will increase the number of required modes.

The amount of modal reduction available is therefore inversely proportional to the number of gear teeth and shaft operating speed.

5.2 Gyroscopic Impacts

The presence of gyroscopics complicates the analysis of any system, and modal synthesis is no different. As previously discussed, a full modal speed-sweep response analysis requires the transformation matrices to be calculated at each speed interval, which greatly adds to computer processing time. Nevertheless, figures 3 and 4 showed that one could reach a good approximation by "fixing" the gyroscopics and calculating the transformation matrices at one speed only. However, the ability to fix the gyroscopics depends upon the system's sensitivity to gyroscopic effects.

5.3 Limitations to Practicality

These two factors may adversely affect the utility of the methodology by increasing the computer processing time of a procedure originally designed to reduce it. A comparison of computing time is presented in table 4, illustrating the gyroscopic effects on processing time. The full 252-DOF system model is the comparison standard with a computer processing ratio of one. In the Full Modal Synthesis models, where the transformation matrices are recalculated for each operating speed within the spectrum, the 168 and 30 DOF models take 8.7 and 5.9 times longer to process, respectively, than the full finite element model. The Modal Fixed Gyro scenarios reduce those times substantially. In the case of the 30 DOF model, the processing time is 20% of the full system model. However, as pointed out, these two reduction models do not produce an accurate gear-mesh frequency response.

Table 4. Vibration response processing time ratio comparison

Degrees of Freedom	**252**	**168**	**30**
Full Modal Synthesis Scenario	1	8.7	5.9
Modal Fixed Gyro Scenario	1	1.3	0.2

Consequently, while this experiment validates the modal synthesis procedure and results in computer processing time savings during eigen analysis, the cutoff frequency or limit of modal reduction is determined by the type of excitation analyzed. Therefore, it may or may not be particularly practical for use in vibration response calculations.

6. Conclusions

This report has presented a method for performing modal synthesis on a geared rotor dynamic system undergoing general damping and gyroscopic effects. The modal analysis produces the eigen solutions, frequency response, and time domain response of the system. Validation of the reduced model occurred by comparing the eigen-solutions and frequency responses of the reduced system with the original model. The results, in almost all instances, matched exactly.

In the speed-sweep response, the modal synthesis procedure resulted in limitations due to the limit of modal reduction imposed by gear-mesh frequency considerations and the amount of computer processing time required. The gear-mesh frequency excited higher modes of vibration, which required a higher DOF model to maintain accuracy. The introduction of gyroscopic effects increased processing time, substantially in some cases. These two limitations call into question the applicability and practicality of using the modal synthesis method for geared, rotating systems.

Finally, an important point is that this was only one system analysis; other systems may behave differently. For example, fixing the gyroscopic speed value in the transformation matrix of this scenario was acceptable. Other systems may be more susceptible to gyroscopic effects, where fixing the speed would be unacceptable. It also may be that in other systems, the ratio of computer processing time is substantially lower for response calculations, making it an attractive alternative to the full finite element model, especially when the full model contains thousands or millions of DOF.

7. Recommendations

Recommended further research falls into three categories. The first deals with application to other systems. This procedure worked very well for a simple, symmetric, two-shaft system. More complex systems might behave differently, especially when gyroscopic sensitivity is considered. Second, the extension of this method in complex notation to capture forward and backward whirl might also be of interest. Finally, this method should be further considered for its potential to other applications, including system identification and design optimization methods.

8. References

1. Hurty, W. Vibrations of Structural Systems by Component Mode Synthesis. *Journal of the Engineering Mechanics Division* **Aug 1960**, Proceedings of the American Society of Civil Engineers, *86* (EM-4), 51–69.

2. Curnier, A. On Three Modal Synthesis Variants. *Journal of Sound and Vibration* **1983**, *90* (4), 527–540.

3. He, J.; Fu, Z. *Modal Analysis*. Woburn, Massachusetts: Butterworth-Heinemann, 2001.

4. Nelson,H.; et al. Nonlinear Analysis of Rotor-Bearing Systems Using Component Mode Synthesis. ASME Paper 82-GT-303, 1982.

5. Johnson, D. Modes and Frequencies of Shafts Coupled by Straight Spur Gears. *Journal of Mechanical Engineering Science* **1962**, *4*, 241–250.

6. Özgüven, H. Twenty Years of Computational Methods for Harmonic Response Analysis of Non-Proportionally Damped Systems. *Proceedings to IMAC-XX: A Conference on Structural Dynamics*, vol. 1 (2002) 390-396. Presented at the 20th International Modal Analysis Conference, Los Angeles, CA, February 2–4, 2002.

7. Yang, B. Exact Receptances of Nonproportionally Damped Dynamic Systems. *Journal of Vibration and Acoustics* **1993**, *115*, 47–52.

8. Zehn, M. A Combination of Modal Synthesis and Subspace Iteration for an Efficient Algorithm for Modal Analysis Within a FE-code. *Shock and Vibration* **2003**, *10*, 27–35.

9. Garvey, S.; Friswell, M.; Prells, U. Coordinate Transformations for Second Order Systems, Part I: General Transformations. *Journal of Sound and Vibration* **2002**, *258* (5), 885–909.

10. Garvey, S.; Friswell, M.; Prells, U. Coordinate Transformations for Second Order Systems, Part II: Elementary Structure-Preserving Transformations. *Journal of Sound and Vibration* **2002**, *258* (5), 911–930.

11. Kessler, C.; Kim, J. Vibration Analysis of Rotors Using Implicit Directional Information of Complex Variable Descriptions. *Journal of Vibration and Acoustics* **2002**, *124*, 340–349.

12. Houlston, P.; Garvey, S.; Popov, A. Modal Control of Vibration in Rotating Machines and Other Generally Damped Systems. *Presented at the ISMA 2006 International Conference on Noise and Vibration Engineering*, Leuven, Belgium, September 18–20, 2006.

13. Luo, Z.; Sun, X.; Fawcett, J. Coupled Torsional-Lateral-Axial Vibration Analysis of a Geared Shaft System Using Substructure Synthesis. *Mechanism and Machine Theory* **1996**, *31* (3), 345–352.

14. Stringer, D.; Sheth, P.; Allaire, P. Gear Modeling Methodologies for Advancing Prognostic Capabilities in Rotary-Wing Transmission Systems. *Proceedings of the American Helicopter Society 64th Annual Forum*, Montreal, Canada, April 30–May 1, 2008.

15. Lim, T.; Singh, R. Vibration Transmission Through Rolling Element Bearings. Part III: Geared Rotor System Studies. *Journal of Sound and Vibration* **1991**, *151* (1), 31–54.

16. Choy, F.; Ruan, Y.; Zakrajsek, J.; Oswald, F. Modal Simulation of Gearbox Vibration with Experimental Correlation. *Journal of Propulsion and Power* **1993**, *9*, 301–306.

17. Kahraman, A.; Özgüven, H.; Houser, D.; Zakrajsek, J. *Dynamic Analysis of Geared Rotors by Finite Elements*; NASA TM 102349, AVSCOM TM 89-C-006, 1990.

List of Symbols

$[\mathbf{C}]$	general damping matrix
c_{xx}, c_{yy}	bearing damping values in *x* and *y*-directions, respectively
$[\mathbf{D}]$	combined damping/gyroscopic matrix
d_i	diagonal damping matrix component
$\{\mathbf{F}(t)\}$	excitation force vector
$[\mathbf{G}]$	gyroscopic matrix
$[\mathbf{I}]$	identity matrix
j	imaginary component, $\sqrt{-1}$
$[\mathbf{K}]$	stiffness matrix
k_i	diagonal stiffness matrix component
k_{xx}, k_{yy}	bearing stiffness values in *x* and *y*-directions, respectively
$[\mathbf{L}]$	transformation sub-matrix designation
$[\mathbf{M}]$	consistent mass matrix
m_i	diagonal mass matrix component
N	number of degrees of freedom
P	number of reduced degrees of freedom
$\{\mathbf{Q}\}$	amplitude of physical coordinate vector of general equation of motion
$\{\mathbf{q}\}$	physical coordinate vector
$\{\dot{\mathbf{q}}\}$	first derivative of physical coordinate vector
$\{\mathbf{u}\}$	first derivative of principal coordinate vector

$\{\mathbf{v}\}$	principal coordinate vector
$[\mathbf{A}_i]$	original state-space matrix
$[\mathbf{B}_i]$	transformed state-space matrix
$[\mathbf{T}]$	transformation matrix
Ω	shaft rotational speed
α	real eigenvalue component
β	imaginary eigenvalue component
$[\mathbf{\Gamma}]$	diagonalizing matrix
ζ	damping ratio
$[\mathbf{\Lambda}]$	diagonal eigenvalue matrix
λ	complex eigenvalue
$[\mathbf{\Xi}]$	elimination matrix
$[\mathbf{\Phi}]$	reduced system modal matrix
$[\mathbf{\Psi}]$	original modal matrix
$\{\boldsymbol{\varphi}\}$	eigenvector
ω	system frequency

Subscripts

D	diagonal
Dm	transformed mesh
l	left
m	number of substructures of global system
$mesh$	gear-mesh
n	natural frequency
r	right
sys	global system to include coupling effects

Superscripts

T	transpose
'	first-order vector, scaled or normalized
*	global system excluding coupling effects

No. of Copies	Organization
1 ELEC	ADMNSTR DEFNS TECHL INFO CTR ATTN DTIC OCP 8725 JOHN J KINGMAN RD STE 0944 FT BELVOIR VA 22060-6218
1	DARPA ATTN IXO S WELBY 3701 N FAIRFAX DR ARLINGTON VA 22203-1714
1 CD	OFC OF THE SECY OF DEFNS ATTN ODDRE (R&AT) THE PENTAGON WASHINGTON DC 20301-3080
1	US ARMY RSRCH DEV AND ENGRG CMND ARMAMENT RSRCH DEV AND ENGRG CTR ARMAMENT ENGRG AND TECHNLGY CTR ATTN AMSRD AAR AEF T J MATTS BLDG 305 ABERDEEN PROVING GROUND MD 21005-5001
1	US ARMY TRADOC BATTLE LAB INTEGRATION & TECHL DIRCTRT ATTN ATCD B 10 WHISTLER LANE FT MONROE VA 23651-5850
1	PM TIMS, PROFILER (MMS-P) AN/TMQ-52 ATTN B GRIFFIES BUILDING 563 FT MONMOUTH NJ 07703
1	US ARMY INFO SYS ENGRG CMND ATTN AMSEL IE TD F JENIA FT HUACHUCA AZ 85613-5300
1	COMMANDER US ARMY RDECOM ATTN AMSRD AMR W C MCCORKLE 5400 FOWLER RD REDSTONE ARSENAL AL 35898-5000
5	NASA GLENN ATTN AMSRD ARL VT D STRINGER 21000 BROOK PARK RD MS 501-2 CLEVELAND OH 44135-3191
1	US GOVERNMENT PRINT OFF DEPOSITORY RECEIVING SECTION ATTN MAIL STOP IDAD J TATE 732 NORTH CAPITOL ST NW WASHINGTON DC 20402
1	US ARMY RSRCH LAB ATTN AMSRD ARL CI OK TP TECHL LIB T LANDFRIED BLDG 4600 ABERDEEN PROVING GROUND MD 21005-5066
1	DIRECTOR US ARMY RSRCH LAB ATTN AMSRD ARL RO EV W D BACH PO BOX 12211 RESEARCH TRIANGLE PARK NC 27709
3	US ARMY RSRCH LAB ATTN AMSRD ARL CI OK PE TECHL PUB ATTN AMSRD ARL CI OK TL TECHL LIB ATTN IMNE ALC IMS MAIL & RECORDS MGMT ADELPHI MD 20783-1197
5	UNIVERSITY OF VIRGINIA DEPT OF MECH & AERO ENGR ATTN P SHETH PO BOX 400746 MECH. ENGR. BLDG 208-B CHARLOTTESVILLE VA 22904
5	UNIVERSITY OF VIRGINIA DEPT OF MECH & AERO ENGR ATTN P ALLAIRE PO BOX 400746 MECH. ENGR. BLDG 208-B CHARLOTTESVILLE VA 22904